Arch. Mech., 44, 2, pp. 171–190, Warszawa 1992

The experimental verification of the unloading technique for the yield surface determination

W. TRĄMPCZYŃSKI (WARSZAWA)

USING THE TECHNIQUE of successive unloadings (proposed by the author in [1, 2]), the standard physical quantities and the stress jump corresponding to opposite direction of plastic straining can be measured. Such data enable us to get, in a simplified way, certain information on the material yield surface. In the case of the Huber–Mises yield surface even its radius and position of the surface center can be detected in this way. In the present paper the yield surfaces were determined for different loading histories, using one specimen yield surface "punching" technique. These results were compared with that obtained by using the simplified procedure mentioned above. Experiments were performed on thin tube specimens made of 18G2A steel under monotonic tension and torsion, cyclic tension – compression and cyclic opposite torsion-proportional loadings. It is shown that the unloading technique can be very useful in determining the yield surface main properties, even in the case of complicated loading histories.

1. Introduction

THE ACCURATE DESCRIPTION of solids behavior under various loadings plays an important role in engineering applications, and several theories have been proposed to describe it [e.g. 3–6]. They were constructed on the basis of the existing experimental results, but none of them covers all the phenomena observed. So, new experimental results and new theoretical ideas have to be developed.

The experiments concerning the yield surface determination have been carried out by several authors [e.g. 7–12]. Because of technical difficulties connected with obtaining the well defined and homogeneous stress state in the three-dimensional case, experiments are usually conducted under plane stress conditions. The different ways of specimens loading can be represented [2, 13] by planes intersecting the Huber–Mises potential. The ellipses obtained in this manner visualize the stress state which is realized by means of different experimental techniques, such as tension–torsion, tension–internal pressure, tension–torsion–internal pressure and torsion of thin tubular specimens. Any of the testing methods mentioned above gives only a limited amount of information concerning the material behavior in the whole stress space, and the results have to be treated as complementary. It can be assumed that tension–torsion tests of thin tubular specimens are mostly used. In such a case the way of the yield surface determination is schematically shown in Fig. 1. The yield surface is defined by experimental determination of several yield points. The specimens are loaded by different τ_{xy}, $\sigma_x(\gamma_{xy}, \varepsilon_x)$ ratios, up to the yield limit defined usually as the stress state corresponding to a certain plastic strain value [7]. Such a technique can be realized in two ways:

the entire yield surface is determined by means of one specimen and the consecutive yield points are defined by a slight surface "punch".

every yield point on the yield surface is determined by means of one specimen.

The first technique, mentioned above, can be applied when the yield limit is defined as that corresponding to a small amount of plastic strains. It is due to the fact that

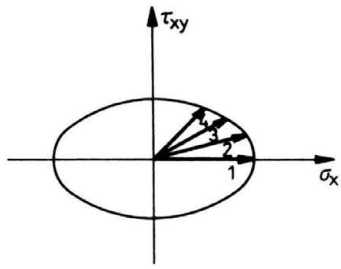

FIG. 1. Determination of the subsequent yield surface points.

every yield surface "punch" adds some plastic strains to the plastic loading history. So, determination of several points can disturb this history. Thus, the amount of the yield surfaces defined during the loading program is quite limited, and the data obtained can prove to be insufficient for the detecting material parameter evolution in the case of more complicate loading histories.

The second technique is quite expensive (large number of specimens is needed) and all data obtained in this way contain a scatter due to different properties of different specimens.

In both cases the determination of yield surface is a laborious, technically difficult and costly task. In the case of more complicated loading histories, when the yield surface has to be defined in several points, particularly difficult and expensive program must be carried out.

After all, the experimental results obtained until now are still inconclusive. Although it is quite well established that the yield surface for the metals in the virgin state can be described by the Huber–Mises potential, the shape of the yield surface for plastically prestrained material depends very much on the assumed yield definition (for example, in Fig. 15 the yield surfaces for copper after 17% of shear are shown [16]. The dashed line refers to the "small" offset definition, and the solid one – to the back extrapolation technique). So, new experimental results are expected. First of all experiments concerning the behavior of material yield surface under more complicated loading histories (e.g. cyclic loading, non-proportional loading, etc.) are needed.

A much simplified technique of determination of the yield surface was proposed in [1, 2]. Using this technique it is possible to detect, in a simple way, two well-defined points on the yield surface. These two points can then be used for theoretical verification. In the case of the Huber–Mises yield surface, these two points give enough data for determination of the whole surface. Let us now summarize the main idea of this technique.

Most of the theoretical models in plasticity employ the notion of a yield function f, which can be written in the following form:

$$f(S_{ij} - \alpha_{ij}, H) = 0, \quad f(0, H) <= 0, \tag{1.1}$$

where α_{ij} ($\alpha_{kk} = 0$) is sometimes identified with a macroscopic measure of microstresses, S_{ij} ($S_{kk} = 0$) denote the deviatoric part of the stress tensor σ_{ij} and H describes the history of plastic strains. Equation (1.1) can be presented in the equivalent parametric form:

$$S_{ij} - \alpha_{ij} = n_{ij} R(n_{ij}, H), \tag{1.2}$$

where n_{ij} is the unit "vector" of directions in S_{ij} space ($n_{ij} n_{ij} = 1$, $n_{ii} = 0$).

For regular yield conditions R is a differentiable function of n_{ij} and H. It can be assumed that f occurring in Eq. (1.1) is so chosen that:

$$\partial f/\partial S_{ij} \times \partial f/\partial S_{ij} = 1 \quad (f = 0), \tag{1.3}$$

hence, the associated plastic flow can be written as:

$$\dot{e}^p_{ij}/(\dot{e}^p_{mn}/\dot{e}^p_{mn})^{1/2} = \partial f/\partial S_{ij}. \tag{1.4}$$

Let us assume now the process of proportional plastic straining

$$e^p_{ij} = m_{ij}e^p(t), \quad m_{ij}m_{ij} = 1, \quad m_{kk} = 0 \tag{1.5}$$

such that $e^p(0) = 0$, $\dot{e}^p(0) > 0$ and the specimens are initially in the annealed state ($H = 0$, $\alpha_{ij} = 0$). Substituting Eqs. (1.5) and (1.2) into Eq. (1.4) one obtains the formal relationship between m_{ij} and n_{ij}:

$$m_{ij}(\operatorname{sgn}\dot{e}^p) = F_{ij}(n_{ij}, H), \quad F_{ij} = \partial f/\partial S_{ij} \tag{1.6}$$

from which it follows that m_{ij} is a unique function of n_{ij} for every H provided that $\dot{e}^p$ does not change sign. It can be assumed also that n_{ij} is a unique function of m_{ij}. Let us introduce now the length λ of the plastic strain trajectory as an independent variable instead of the real time

$$\lambda = \int_0^t |\dot{e}^p|\, dt. \tag{1.7}$$

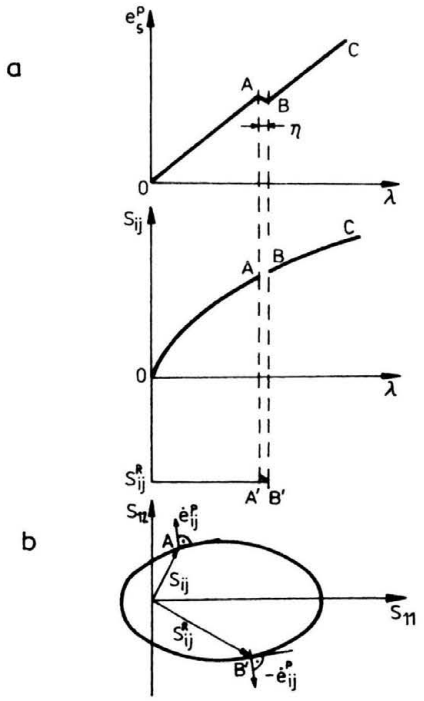

FIG. 2. Theoretical basis for the two yield points technique.

The basic program O-C of plastic straining is shown in Fig. 2a. The loading is interrupted at point $A(S_{ij})$ where specimen is unloaded and then reloaded into reverse straining direction until the small value of the increment of $\dot{e}^p$ (the yield definition) is achieved (S_{ij}^R) (Fig. 2b.). One end of the stress deviator (S_{ij}^R) lies on the yield surface at point B', where the plastic strain-rate vector has the direction opposite to that prescribed in the basic program. In this moment the reloading process is stopped, the specimen is unloaded and loaded in former direction. The basic straining program is then continued. In this way two well defined points S_{ij} and S_{ij}^R on the current yield surface are obtained, for the chosen plastic strain history described by λ (it is assumed that the plastic strain increment due to point B' identification is negligible). The first point lies on the yield surface where the plastic strain rate vector has the direction prescribed by the basic program, and the second one lies on the yield surface where the plastic strain rate vector has the opposite direction. Because of simplicity of this technique and because of the fact that it is only one yield surface "punch", it can be used several times during the whole loading history. Even for quite complicated loading histories (e.g. cyclic ones) the evolution of such parameters as:

$$\begin{aligned} Y_{ij} &= (S_{ij} - S_{ij}^R)/2, \\ \Pi_{ij} &= (S_{ij} + S_{ij}^R)/2, \end{aligned} \tag{1.8}$$

can follow and then they can be used for experimental comparison of theoretical predictions.

Assuming that the current yield surface can be approximated by a second order surface possessing the centre of symmetry (ellipsoids), it is possible to show [1] that

$$\begin{aligned} Y_{ij} &= (S_{ij} - S_{ij}^R)/2 = n_{ij} R(n_{ij}, H), \\ \Pi_{ij} &= (S_{ij} + S_{ij}^R)/2 = \alpha_{ij}. \end{aligned} \tag{1.9}$$

In a particular case when the successive yield surfaces are approximated by the Huber–Mises spheres, then

$$\begin{aligned} Y_{ij} &= (S_{ij} - S_{ij}^R)/2 = n_{ij} R(H), \\ \Pi_{ij} &= (S_{ij} + S_{ij}^R)/2 = \alpha_{ij}. \end{aligned} \tag{1.10}$$

So, in such a case one can experimentally determine not only the evolution of Y_{ij} and Π_{ij}, but also the evolution of the yield surface radius (R) and the position (α_{ij}) of its center.

The technique mentioned above was used for determination of Y_{ij} and Π_{ij} in the case of cyclic loading, for two kind of steels [1, 14]. Then in [15] Huber–Mises material yield surface was assumed and the theoretical description was proposed to describe the evolution of R and α_{ij} due to different loading histories.

Now the question arises, to what extent this simplified technique can be used for determination of the main properties of the yield surface.

The present paper gives some information concerning that question. The experimental results are reported where, for the proportional loading programs similar to that presented in [1, 14], the yield surface obtained by one specimen "punching" technique is compared with the results obtained by the unloading technique. Several propositions for interpretation of the experimental data (obtained by this simplified technique) are given.

2. Experimental investigation

The experimental programs were performed on thin tubes (outer diameter 24 mm, wall thickness 2 mm) made of 18G2A steel at room temperature. Tension-compression and opposite torsion cyclic programs were performed using the facilities of the Institute of Mechanics 1 of Bochum University, described in [1]. All programs were performed with a constant effective strain rate $\dot{e}_e = 3.4 \cdot 10^{-4}\text{s}^{-1}$, and the actual stress versus the logarithmic plastic strain were calculated and plotted.

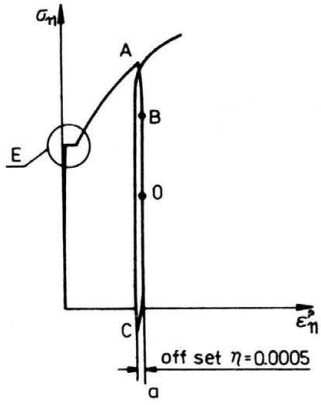

FIG. 3. Application of the "offset" yield technique in the case of tension.

The yield points were defined by the offset definition $\eta = 0.0005$ as it is shown in Fig. 3 in the case of tension loading (in the case of complex stresses the curves σ_e versus e_e were used). At a chosen moment of plastic strain history the value of the stress deviator S_{ij} was recorded, the straining direction was reversed and the slope of unloading curve was measured. At point B this slope was equal to Young's modulus for the virgin material and the straight line a of the same slope was determined. The distance between the successive points on the unloading curve (loading in "opposite" direction) and on this straight line was then calculated. When it was equal to the value η (the "offset definition" of the yield point), the second yield point S_{ij}^R was found and the strain direction was changed to the former one. Then the middle point $0 = (S_{ij} + S_{ij}^R)/2$ was determined and other points on the yield surface were searched in the way shown in Fig. 4, with point 0 being the center point. So, the presented technique of determination of the yield "offset" was used for all points shown in Fig. 4, starting from the center point 0. At the end the primary direction of the strain rate was applied and the prescribed loading program was continued.

Because of the instable behavior of the curve σ versus e for this material (Fig. 3 — region E), all the specimens were primarily prestrained up to $e^p = 0.003$ in tension, compression and opposite torsion. So, all the specimens were primarily preloaded with $e_e^p = 1.2\%$.

As it was mentioned before, in the case of the one specimen "punching" technique, determination of every yield point adds some plastic strain value due to the yield definition. For the presented experimental program the "offset" definition $\eta = 0.0005$ was assumed. So, detecting eleven (the last 12th one was used for control) separate yield

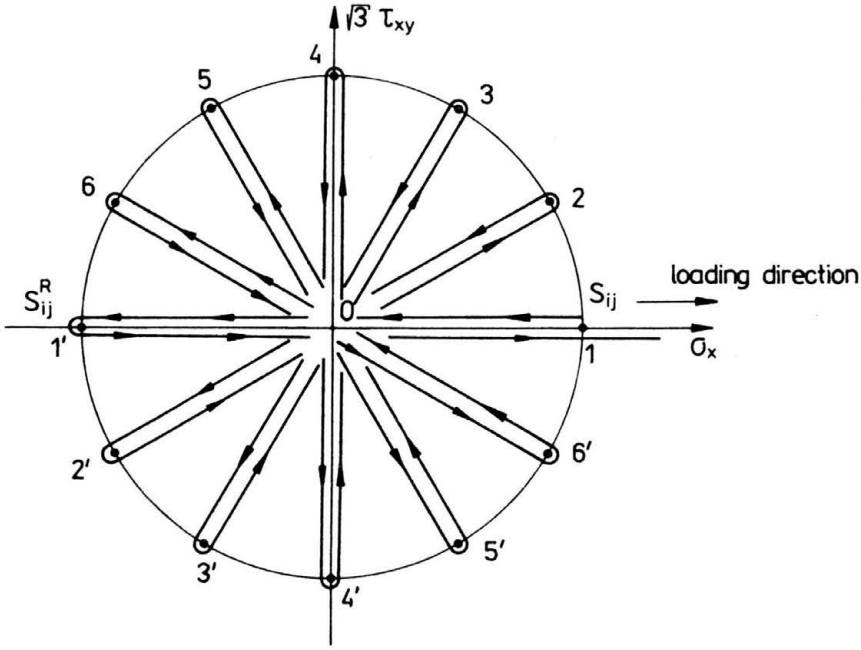

FIG. 4. Determination of the yield surface.

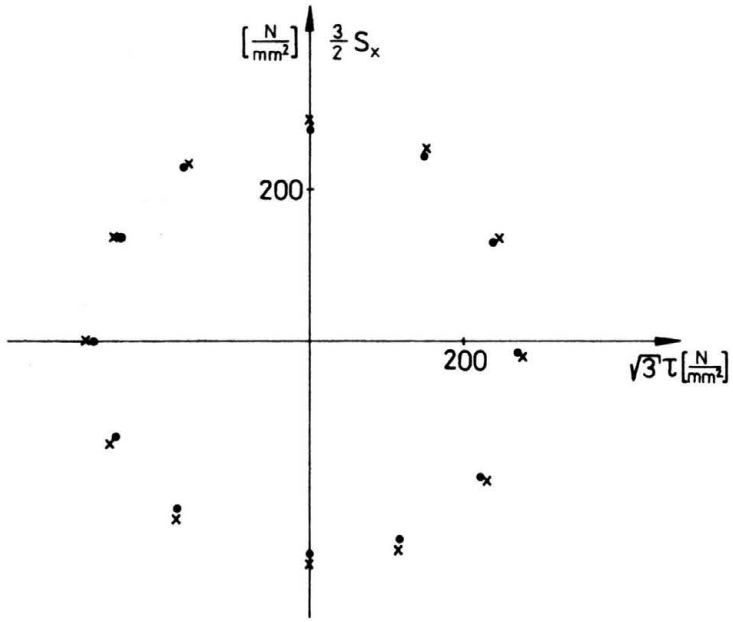

FIG. 5. The virgin material yield surface determined by two following procedures (1th procedure — •, 2nd procedure — x).

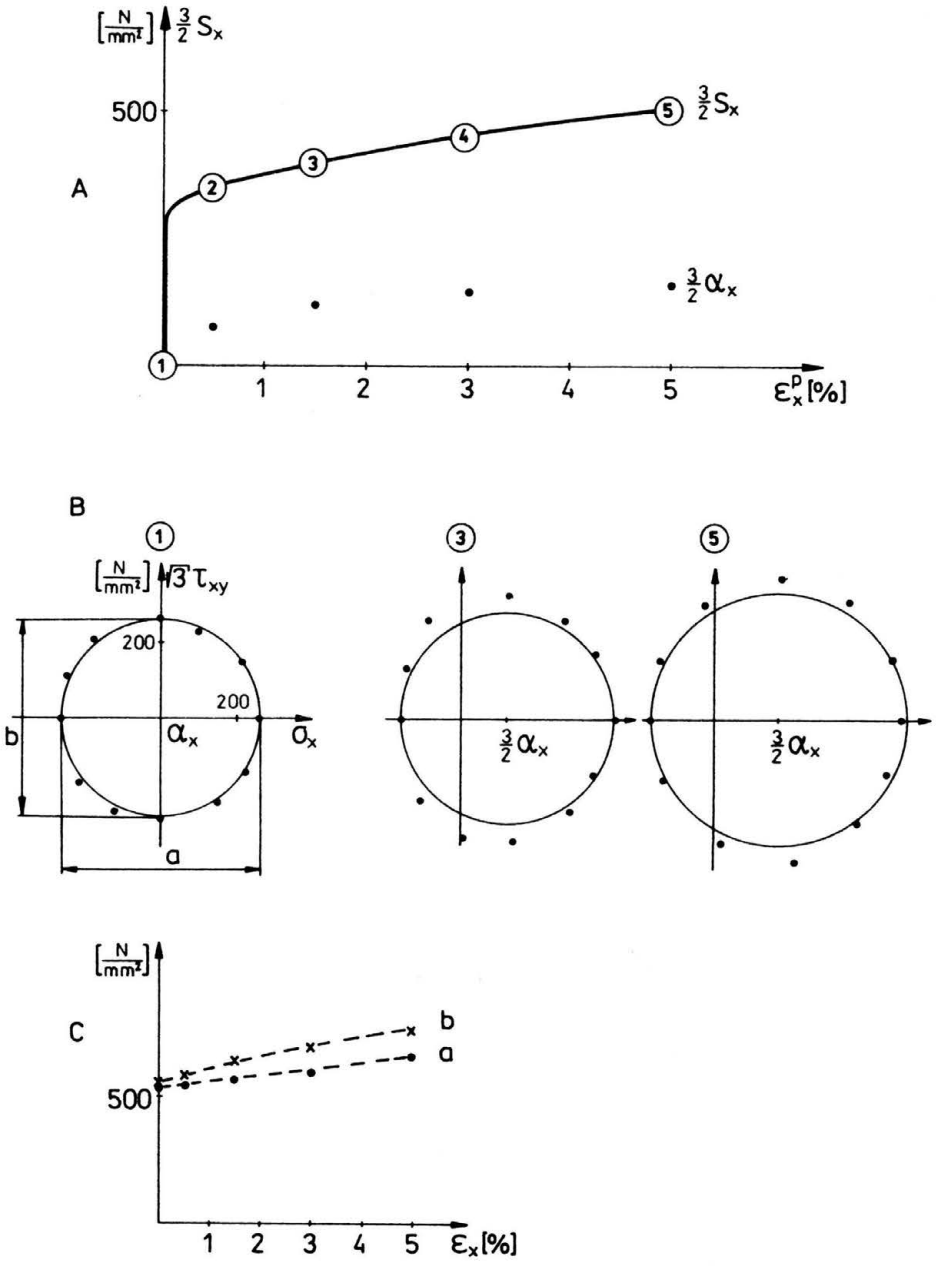

FIG. 6. Monotonic loading under tension with subsequent yield surface determination.

points, the additional effective plastic strain $e_e^p = 0.006$ was imposed for every yield surface determination procedure. The influence of such a plastic strain increment on the form of the yield surface is shown in Fig. 5. The yield surface (for the virgin material) was detected twice (• — points of the first yield surface, × — points of the second yield

surface, obtained just after the first one). It is shown that in spite of a slight change in the surface size, its shape doesn't change.

Experiment 1. Monotonic loading under tension

The specimen was loaded by tension at the constant effective strain rate $\dot{e}_e = 3.4 \cdot 10^{-4}\text{s}^{-1}$. After the assumed plastic strain increment Δe_e^p, the yield surface was determined using the one specimen "punching" technique (Fig. 6A, B; Fig. 6B showns the obtained yield surfaces). The evolution of two main yield surface dimensions is shown in Fig. 6C. Although it is shown that the yield surface shape doesn't coincide with the Huber–Mises one (Fig. 6B) (in these coordinates it should be a circle), its two main dimensions (a, b) grow up simultaneously. The maximal value of the distortion parameter $d = 100 \times (b - a)/a = 19$ (Fig. 6B–3).

Experiment 2. Monotonic tension ($\varepsilon_x^p = 5\%$) followed by cyclic tension-compression ($\varepsilon_x^p = \pm 1.5\%$).

The specimen was monotonically loaded by tension up to $\varepsilon_x^p = 5\%$ and then cyclically loaded by tension-compression ($\varepsilon_x^p = \pm 1.5\%$) (Fig. 7). The yield surfaces were determined in three moments of the loading history mentioned (Fig. 7A). The yield surface resulting from the monotonic loading is of the same shape as that resulting from the cyclic loading (Fig. 7B–2, 3). The maximal distortion parameter $d = 100 \times (b - a)/a = 15$.

Experiment 3. Cyclic tension — compression loading with different cyclic amplitude

The specimen was cyclically loaded under tension-compression with ($\varepsilon_x^p = \pm 0.5\%$) cyclic amplitude up to the steady state. Then the amplitude was changed to ($\varepsilon_x^p = \pm 1.5\%$) and the new steady state was achieved. This loading was followed by ($\varepsilon_x^p = \pm 0.5\%$), tension-compression cycling, also up to the steady state. The yield surfaces were determined for all cyclic amplitudes under steady state conditions (Fig. 8A). The shapes of the yield surfaces resulting from the cyclic loading are similar to those resulting from the monotonic one (Fig. 8B). The evolution of two main yield surface dimensions is shown in Fig. 8C. The maximal distortion parameter $d = 100 \times (b - a)/a = 18$.

Experiment 4. Cyclic tension — compression loading with ($\varepsilon_x^p = \pm 1.5\%$) plastic strain amplitude

The specimen was cyclically loaded under tension-compression with ($\varepsilon_x^p = 1.5\%$) amplitude up to the steady state. The yield surfaces were determined at steady state for different plastic strain values ($\varepsilon_x^p = -1.4\%$, $\varepsilon_x^p = 0\%$, $\varepsilon_x^p = +1.4\%$) (Fig. 9A) . The yield surface detected for $\varepsilon_x^p = 0\%$ (Fig. 9B-3) and $\varepsilon_x^p = +1.4\%$ (Fig. 9B–4) have similar shape; it means that they are flattened in the direction "opposite" to the actual plastic strain and have a "nose" in the actual straining direction. The strong cross-effect is observed. The yield surface at point ($\varepsilon_x^p = -1.4\%$) is symmetric (it has a center of symmetry). The main yield surface dimensions (a, b) are almost constant (Fig. 9–C). The maximal distortion parameter was found to be $d = 100 \times (b - a)/a = 24$.

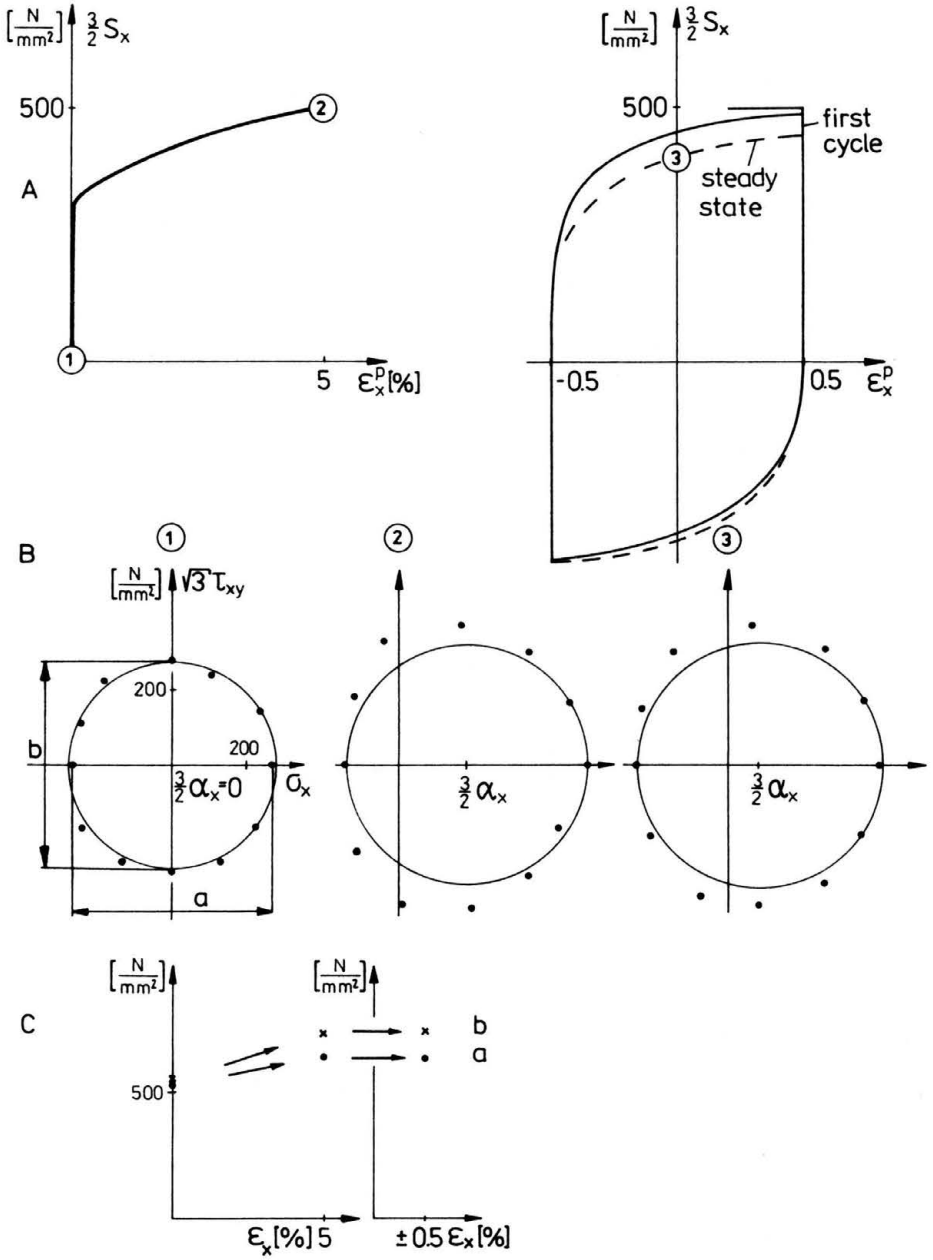

FIG. 7. Monotonic tension followed by cyclic tension-compression.

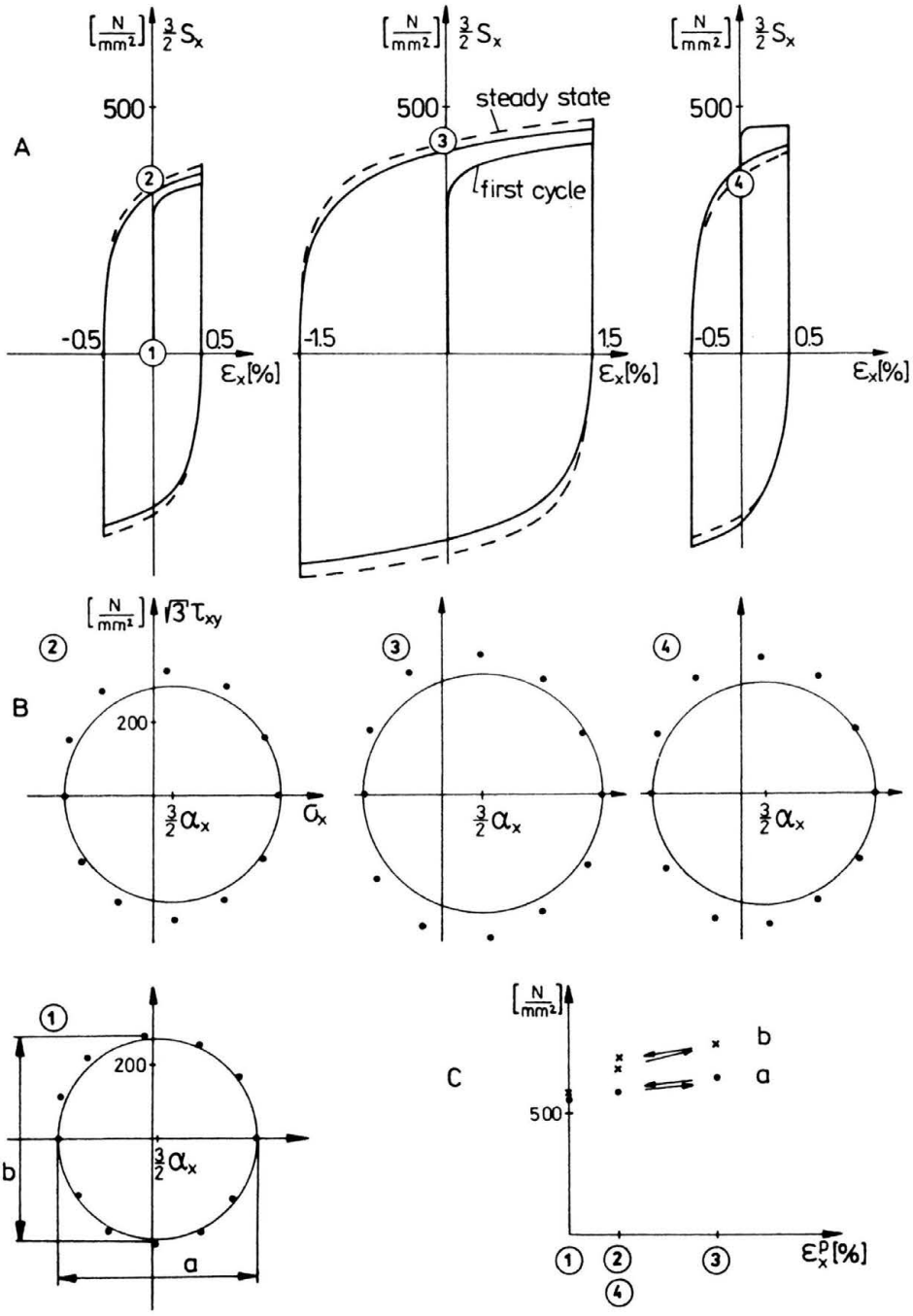

FIG. 8. Cyclic tension-compression loading for different cyclic amplitude.

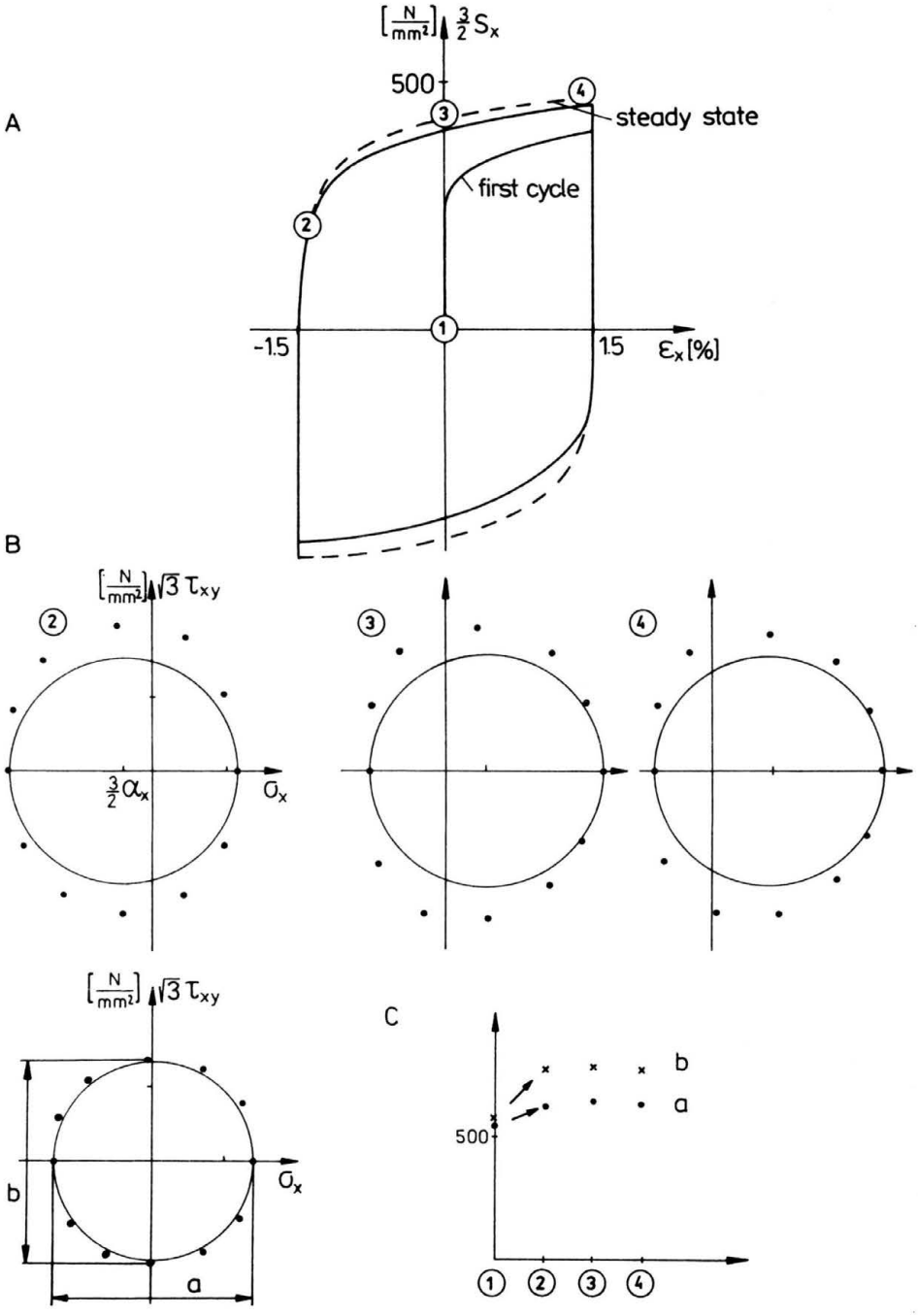

FIG. 9. Cyclic tension-compression loading with $\varepsilon_x^p = \pm 1.5\%$ amplitude.

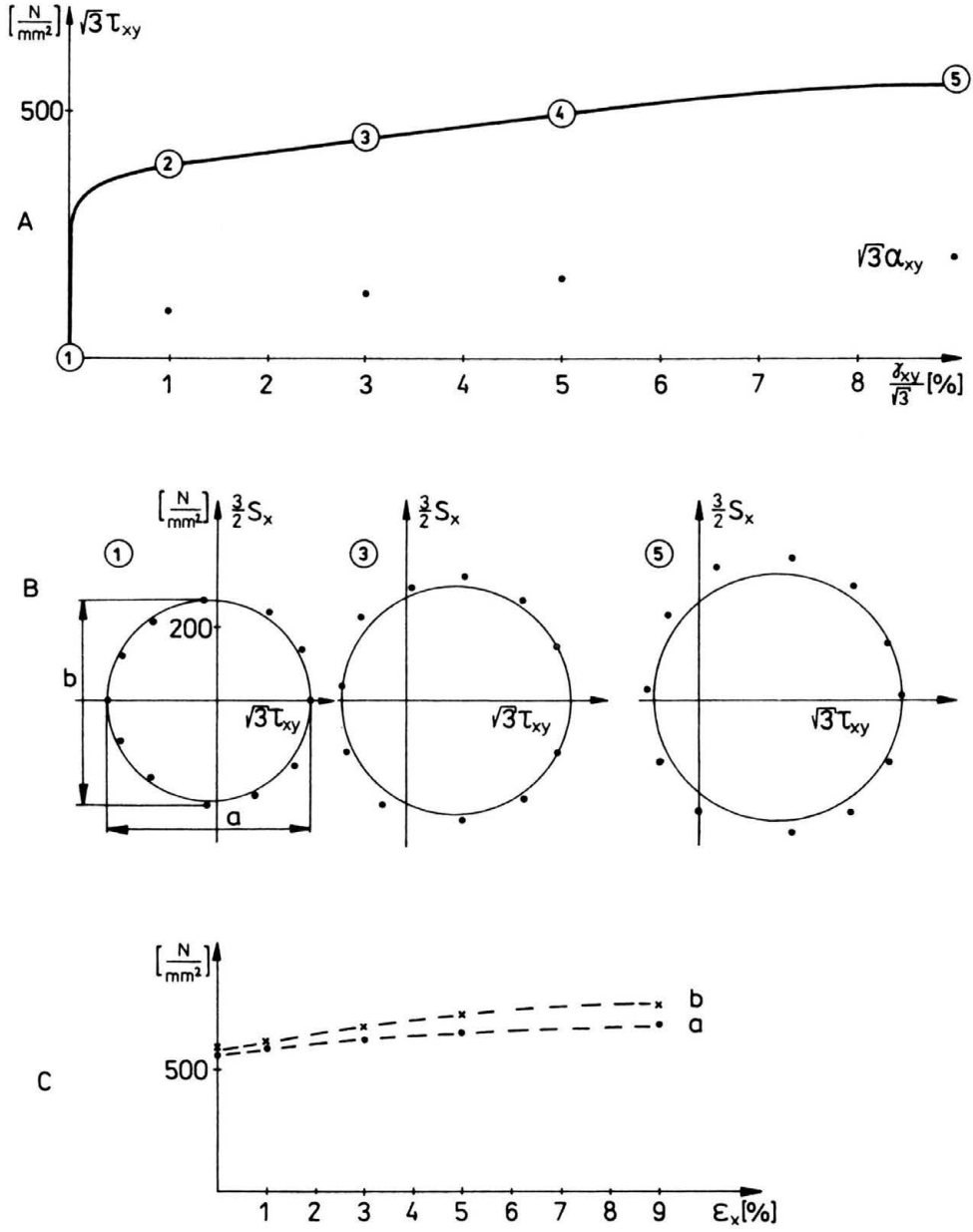

FIG. 10. Monotonic loading under torsion with subsequent yield surface determination.

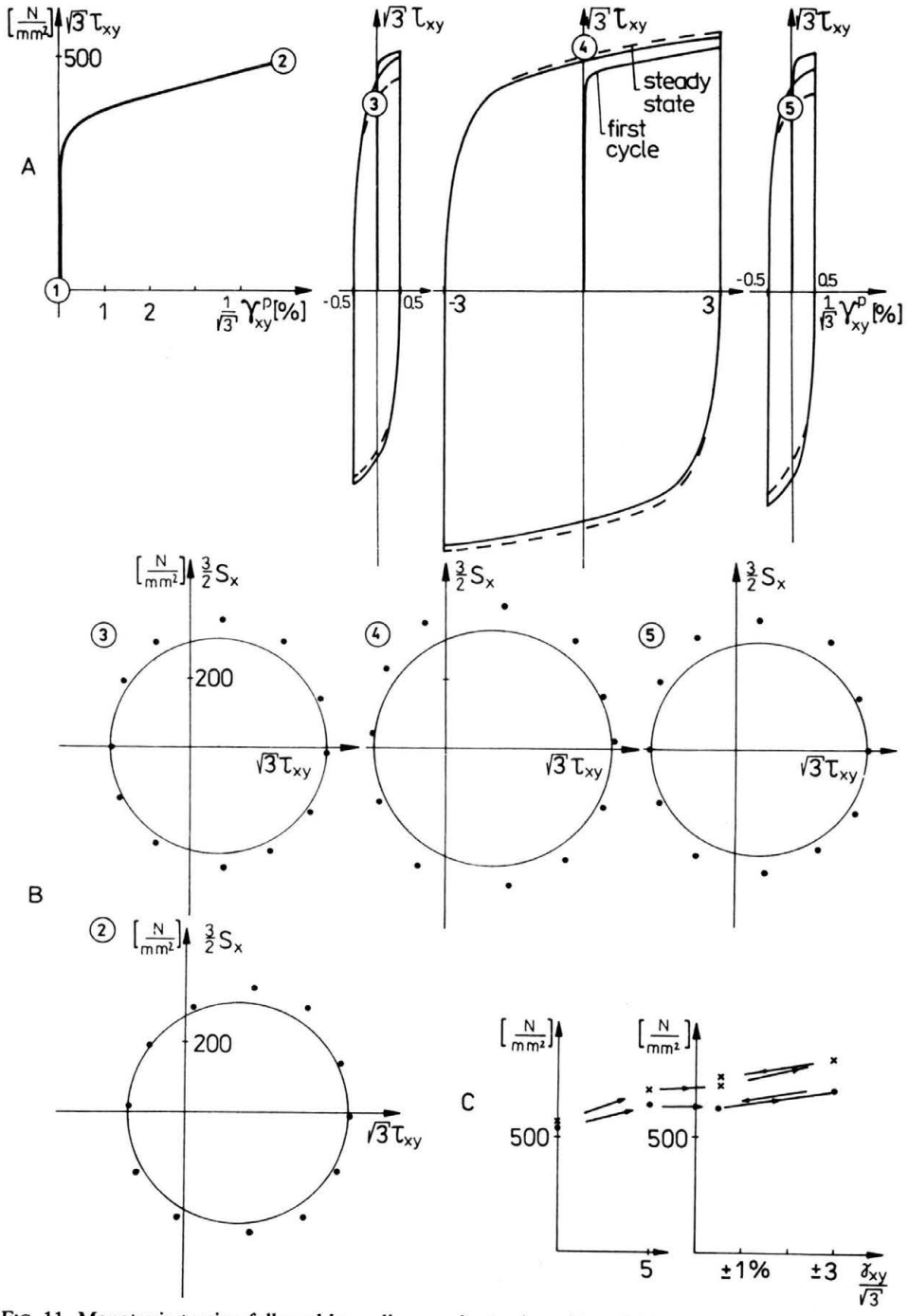

FIG. 11. Monotonic torsion followed by cyclic opposite torsion with variable plastic strain amplitude.

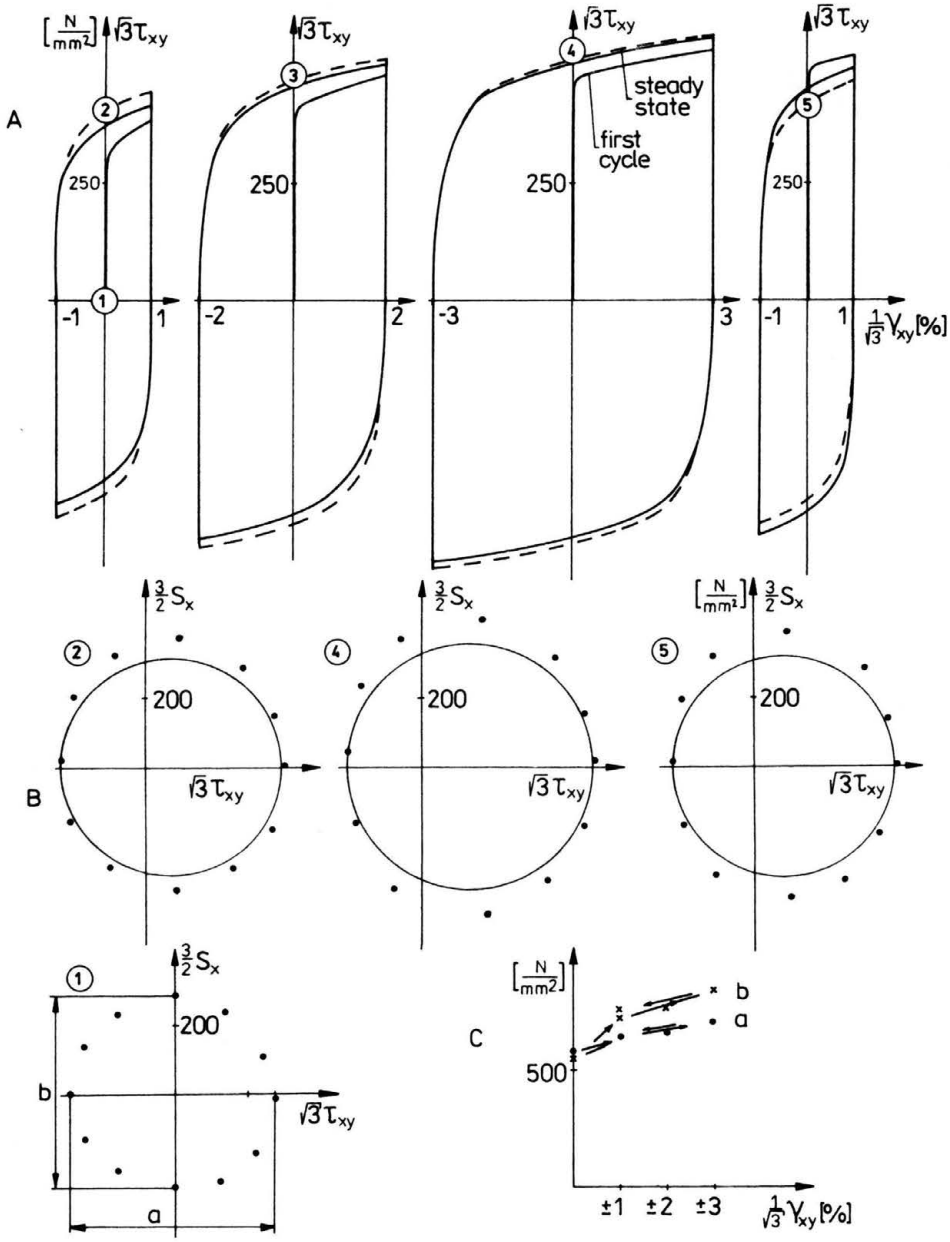

FIG. 12. Cyclic opposite torsion loading with various plastic strain amplitudes.

Experiment 5. Monotonic loading under torsion

The specimen was loaded by torsion at the constant effective strain rate $\dot{e}_e = 3.4 \cdot 10^{-4}\text{s}^{-1}$. In several points of the loading history the yield surface was determined (Fig. 10A) using the one specimen "punching" technique (Fig. 10B — shows the obtained yield surfaces). The evolution of two main yield surface dimensions is shown in Fig. 10C.

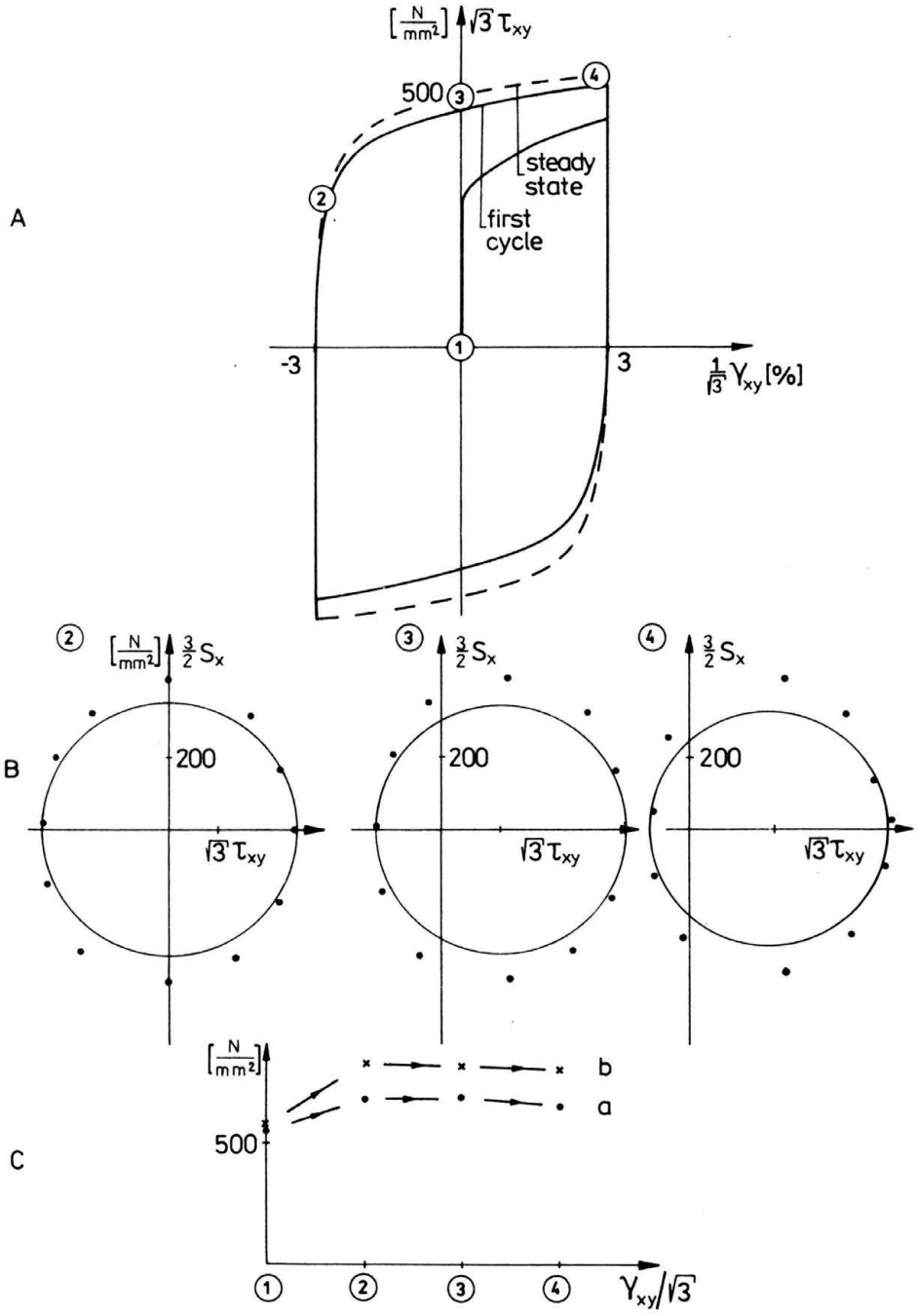

FIG. 13. Cyclic opposite torsion loading with $\gamma^p_{xy}/\sqrt{3} = \pm 3\%$ plastic strain amplitude.

The maximal value of distortion parameter was found to be $d = 100 \times (b - a)/a = 13$.

Experiment 6. Monotonic torsion followed by cyclic opposite torsion with different plastic strain amplitude

The specimen was monotonically loaded by torsion up to $\gamma_{xy}^p/\sqrt{3} = 5\%$ and then cyclically loaded by opposite torsion with variable plastic strain amplitude ($\gamma_{xy}^p/\sqrt{3} = \pm 0.5\%, \pm 3\%, \pm 0.5\%$). The yield surfaces were determined in different moments of the loading history (Fig. 11A, B; Fig. 11B shows the obtained yield surfaces). In the case of cyclic loading it was always the steady state loop when the yield surfaces were searched. The evolution of two main surface dimensions is shown in Fig. 11C. The maximal value of distortion parameter was found to be $d = 23$.

Experiment 7. Cyclic opposite torsion loading with various plastic strain amplitudes

The specimen was cyclically loaded by opposite torsion with the following plastic strain amplitudes: $\gamma_{xy}^p/\sqrt{3} = \pm 1, \pm 2, \pm 3, \pm 1[\%]$. The amplitude change took always place after the steady state loop had been reached (Fig. 12A). The yield surfaces were determined for all cyclic amplitudes under the steady state conditions (Fig. 12B shows the determined yield surfaces). The evolution of two main surface dimensions is shown in Fig. 12C. The maximal value of distortion parameter was found to be $d = 20$.

Experiment 8. Cyclic opposite torsion loading with $\gamma_{xy}^p/\sqrt{3} = \pm 3\%$ plastic strain amplitude

The specimen was cyclically loaded under opposite torsion with $\gamma_{xy}^p/\sqrt{3} = \pm 3\%$ plastic strain amplitude up to the steady state (Fig.13A). The yield surfaces were determined for different plastic strain values ($\gamma_{xy}^p/\sqrt{3} = -2.8\%, 0\%, 2.8\%$) (Fig. 13B — the detected yield surfaces). In spite of the observed change of the yield surface shape, its main dimensions (a, b) are almost constant (Fig. 13C). The maximal distortion parameter was found to be $d = 23$.

3. The experimental results

The complicated proportional plastic strain loading programs, under plane stress conditions, were performed on thin steel tubes under monotonic tension, cyclic tension — compression, monotonic torsion and cyclic opposite torsion loading. The material yield surfaces were determined using one specimen "punching" technique at different instants of the strain history. The following main conclusions can be drawn up:

1. All the results obtained for tension and cyclic tension — compression tests are similar to those resulting from the torsion and cyclic opposite torsion programs.

2. The material yield surface for tension (torsion) and cyclic tension — compression (opposite torsion) loading tests are of the same shape and proportions.

3. The material yield surface can be considered to be the Huber–Mises one (in the assumed coordinates — the circle) only for virgin specimens. Then, it flattens in the direction "opposite" to the actual plastic strain and gets a "nose" in the loading direction. The considerable cross-effect is observed. The surface has no longer the center of symmetry but it is symmetrical to the actual straining direction (Fig. 14/I).

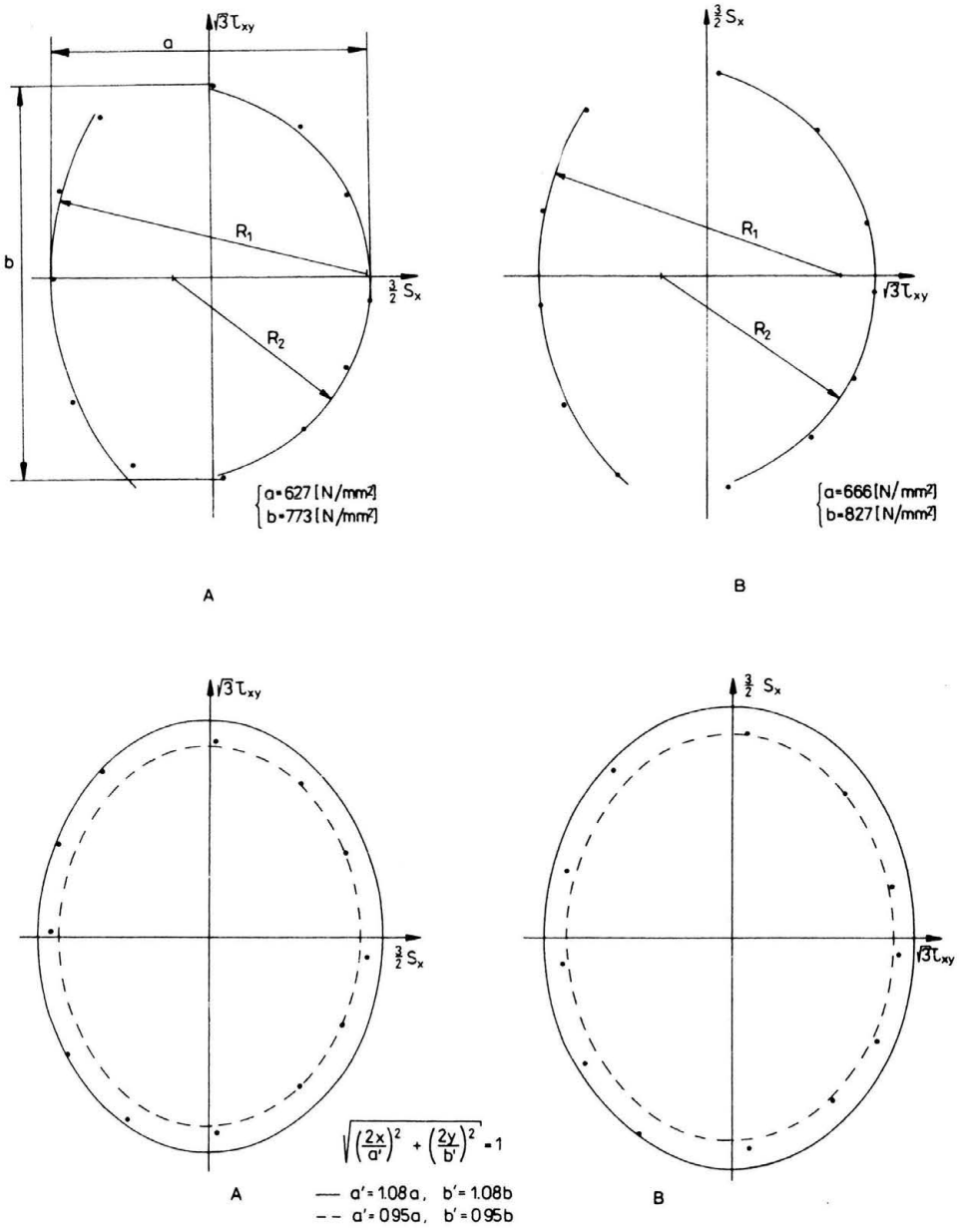

FIG. 14. The chosen material yield surfaces. A — For cyclic tension-compression loading ($\varepsilon_x^p = \pm 1.5\%$) under steady state conditions, when the strain $\varepsilon_x^p = 1.4\%$ is achieved (Fig. 9). B — For opposite torsion loading ($\gamma_{xy}^p/\sqrt{3} = \pm 3\%$) under steady state conditions, when the strain $\gamma_{xy}^p/\sqrt{3} = 2.8\%$ is achieved (Fig. 13).

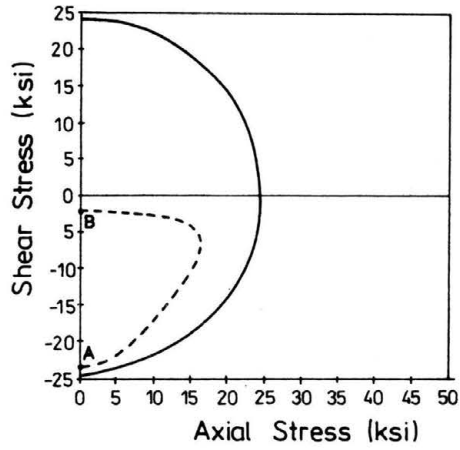

FIG. 15. The yield surface of copper prestrained by torsion up to 17% (- - - - the small offset yield definition, —— the back extrapolation technique).

4. The change of the shape of the material yield surface was presented using two parameters a and b. The first one is the yield surface dimension in the direction of the actual plastic strain and the second one shows its transversal dimension. Both parameters evaluate simultaneously through all the imposed plastic strain histories (when a increases then b also increases; when a decreases then b also decreases).

5. The maximal distortion of the shape of the yield surface (from the Huber–Mises shape) described as $d = 100 \times (b - a)/a$ was found to be $d = 24$ (the cross-effect).

6. As it was mentioned before, the yield surface of plastically strained material has no longer the center of symmetry; however, its shape can be fairly well described to within $+8\%$, -5% accuracy by an ellipse. Such comparison is shown in Fig. 14/II in the case of the surfaces showing the largest cross-effect detected in the experimental programs performed (Fig. 14A — for the tension — compression, cyclic loading, Fig. 14B — for the opposite torsion cyclic loading).

7. In the case of cyclic loading (Fig. 9 and Fig. 13) the yield surface shape also undergoes cyclic changes (the "nose" direction) from that corresponding to one loading direction to that corresponding to the "opposite" one (even and odd half cycles numbers). Its main dimensions remain constant (a, b) for the steady state loop.

The results reported in p. 3 and p. 6 coincide with that obtained for SUS 304 Stainless Steel [11, 12].

4. Conclusions

The simplified two-points yield surface determination technique was described and discussed in Sec. 1. It was shown that, by detecting only two well defined points on the yield surface (S_{ij}, S^R_{ij}) one can get quite a lot of information concerning the surface itself. Assuming the form of the Huber–Mises yield surface, even the entire surface can be

determined in this way. The obtained experimental results provide additional arguments to this discussion.

As it was discussed before, the two-points simplified technique makes it possible to determine experimentally the Y_{ij} and Π_{ij} parameters (Eq. (1.8)). The first one corresponds to the yield surface dimension in the actual direction of plastic strain, marked in the present paper as a, and the second one represents the position of the middle point of that dimension. Although it was found that the yield surface for plastically strained material doesn't coincide with the Huber–Mises surface, this two-parameter evolution gives a lot of information about the yield surface itself. So, the proposed technique can be quite useful in future material investigation. Taking into account the obtained experimental results the following conclusions can be drawn:

1. The yield surface plastically strained material doesn't coincide with the Huber–Mises surface. The significant cross-effect was observed and maximal distortion of the yield surface shape (for this experimental program) described as $d = 100 \times (b - a)/a$, was found to be $d_{\max} = 24$ (Fig. 8).

2. Although the detected material yield surface has no center of symmetry, its shape can be described to within the accuracy of $+8, -5\%$ by an ellipse (in the assumed coordinate system). Its center of symmetry coincides with parameter Π_{ij} (Eq. (1.9)) and the proposed technique enables the experimental determination of α_{ij} (kinematic hardening) evolution. Also the evolution of a (Y_{ij}) (one of the yield surface radius) can be determined in this way. Knowing the $a - b$ relation, the yield surface can be determined in this manner for every moment of the loading history, provided the above accuracy is acceptable.

3. The parameters describing two main yield surface dimensions (a, b) evaluate simultaneously. So, the evolution of one parameter, for example a (Y_{ij}), describes the general behavior of the surface, its growth or shrinkage.

4. The material yield surface for monotonic and cyclic loading are of the same shape and proportions. It means that by determining the evolution of the yield surface in the case of monotonic loading (using, for example, one specimen "punching" technique) and knowing only the evolution of parameter a (Y_{ij}) in the case of cyclic loading, the yield surface shape can be "reconstructed".

5. In the case of more complicated shapes of the material yield surface (which cannot be described by a second order surface possessing the center of symmetry – for example Fig. 15, [16] — dotted line), the Two Points Yield Surface Determination Technique (The Successive Unloading Technique) can be also very useful. One can easily determine in this way two well defined points on the yield surface (Fig. 15 – point A and B). So, the evolution of Π_{ij} and Y_{ij} describe the evolution of the middle point (point 1 and 2) and the dimension of the yield surface in the straining direction. It means that the general behavior of the yield surface (its displacement, expansion or shrinkage) can be detected by this method.

Acknowledgment

This work was carried out during the author's visit to Germany sponsored by the Alexander von Humboldt Foundation. The generosity of the Foundation, hospitality of the Institute of Mechanics I at the Bochum University and the assistance offered by prof. O. Bruhns are gratefully acknowledged.

References

1. TH. LEHMANN, B.RANIECKI and W. TRĄMPCZYŃSKI, *The Bauschinger effect in cyclic plasticity*, Arch. Mech., **37**, 6, pp. 643–659, 1985.
2. W. TRĄMPCZYŃSKI, *On a simple experimental technique for the yield surface determination*, Bull. Polish Acad. Sci., Série Techn. Sci, **37**, 7-12, pp. 407–418, 1989.
3. Z. MRÓZ, *On generalized kinematic hardening rule with memory of maximal prestress*, J. Mech. Appl., **5**, 242–260, 1981.
4. J. L. CHABOCHE, *Time independent constitutive theories for cyclic plasticity*, Int. J. Plast., **2**, 2, 149–188, 1986.
5. H. ISHIKAWA and K. SASAKI, *Constitutive modelling of cyclic plasticity considering induced anisotropy*, in: Constitutive Laws for Engineering Materials, [Eds.] C. S. DESAI *et al.*, Elsevier, pp. 581–583, 1987.
6. TH. LEHMANN, *General frame for the definition of constitutive laws for large non-isothermic elastic-plastic and elastic-visco-plastic deformation*, The Constitutive Law in Thermoplasticity, CISM, 1984.
7. K. IKEGAMI, *Experimental plasticity on the anisotropy of metals*, Proc. Euromech Colloquium, 1979, [Ed.] J. P. BOEHLER, 115, 1982.
8. M. ŚLIWOWSKI, *Behavior of stress-strain diagrams for cyclic loading*, Bull. Polish Acad. Sci., Série Sci.Techn., **27**, 115–123, 1979.
9. J. MIASTKOWSKI, W. SZCZEPIŃSKI, *An experimental study of yield surface for prestrained brass*, Int. J. Solids Struct., 1, 189–194, 1965.
10. A. PHILIPS, J. TANG, M. RICCIUTI, *Some new observations on yield surface*, Acta. Mech., **20**, 23–39, 1974.
11. H. ISHIKAWA, K. SASAKI, *Yield surfaces of SUS304 under cyclic loading*, J. Eng. Mat. and Techn., **110**, 364–371, 1988.
12. H. ISHIKAWA, K. SASAKI, *Stress strain relations of SUS304 stainless steel after cyclic preloading*, J. Eng. Mat. and Techn., **111**, 471–423, 1989.
13. W. SZCZEPIŃSKI, *On the effect of plastic deformations on yield conditions*, Arch. Mech. Stos., **15**, 275–293, 1963.
14. W. TRĄMPCZYŃSKI, *The experimental verification of the evolution of kinematic and isotropic hardening in cyclic plasticity*, J. Mech. Phys. Solids, **36**, 4, pp. 417–441, 1988.
15. W. TRĄMPCZYŃSKI and Z. MRÓZ, *Anisotropic hardening model and its application to cyclic loading*, Anisotropy and Localisation of Plastic Deformation, Proc. Plasticity, 91, [Eds.] J. P. BOEHLER and A. S. KHAN, Elsevier Applied Science, 1991.
16. X. WANG, A. S. KHAN and H. YAN, *On subsequent yield surface after finite shear pre-straining*, Anisotropy and Localisation of Plastic Deformation, Proc. Plasticity, 91, [Eds.] J. P. BOEHLER and A. S. KHAN, Elsevier Applied Science, 1991.

POLISH ACADEMY OF SCIENCES
INSTITUTE OF FUNDAMENTAL TECHNOLOGICAL RESEARCH

Received November 13, 1991.